

INVESTIGATION OF CRYSTALLIZATION FOULING ON NOVEL POLYMER COMPOSITE HEAT EXCHANGER TUBES

*H. Glade¹, S. Schilling¹ and T. Orth²

¹ University of Bremen, Engineering Thermodynamics, Badgasteiner Str. 1, 28359 Bremen, Germany,
email: heike.glade@uni-bremen.de

² Technoform Tailored Solutions Holding GmbH, An den Lindenbäumen 17, 34277 Fuldabrück, Germany

ABSTRACT

Metals are common construction materials for heat exchangers. However, metals may suffer from failure due to corrosion, especially in harsh environments. Innovative thermally conductive polymer composite tubes based on polypropylene or polyphenylene sulphide filled with graphite have been developed. Crystallization fouling on metal surfaces has been extensively studied. However, fouling data for polymer surfaces are very limited. In the current study, a stirred vessel test rig and a horizontal tube falling film test rig were used to compare the fouling propensity of the polymer composite tubes and common stainless steel tubes. Experiments were performed with calcium sulphate solutions and mixed salt solutions containing calcium carbonate and calcium sulphate. The induction periods and the fouling resistances over time were measured. The novel polymer composite tubes showed a lower crystallization fouling propensity compared to the stainless steel tubes. The induction period was longer and the reduction of the overall heat transfer coefficient over time was notably lower compared to the metal tubes.

INTRODUCTION

Metals such as stainless steel, copper, nickel and aluminium alloys, or titanium are the most common materials of construction for heat exchangers due to their favourable thermal and mechanical properties. However, metals may suffer from failure due to corrosion and erosion, especially in harsh environments. In addition, they have disadvantages in terms of high weight and high cost and they are prone to fouling, which is the unwanted deposition of materials on the heat transfer surfaces. Thus, it is a major concern of various industries to find alternative materials for heat exchangers that can overcome these disadvantages.

Driven by the high chemical resistance, low weight, great freedom in shaping and low cost of many polymers, considerable attention has been dedicated to the development and implementation of polymer heat exchanger technology for the past decades [1]. However, the major drawback of polymer materials for using them in heat transfer

applications is their very low thermal conductivity between 0.1 and 0.5 W/(m K) [2]. Heat exchangers with polymers are applied in niche markets where only highly corrosion-resistant and very expensive metals can be used and/or where the low thermal conductivity of the polymer will not significantly reduce the overall heat transfer coefficient because the heat transfer coefficient on one side of the heat transfer surface is very low like in energy recovery systems from exhaust gases.

Polymer matrix composite materials open up new opportunities to create a huge number of new material systems with enhanced thermal properties or other unique characteristics that cannot be obtained using a single monolithic material. Composite materials hold tremendous promise for heat exchanger materials, which can be tailored to meet the specific requirements of an application [3].

Polymer composite tubes based on polypropylene (PP) or polyphenylene sulphide (PPS) filled with graphite particles (GR) have been developed by TECHNOFORM, Germany. Filler type, size, shape, morphology, anisotropy, properties of filler-matrix interfaces and processing history have a strong influence on the thermal conductivity of the composite material [2]. The thermal conductivity significantly increases with the amount of filler, when thermally conductive pathways start to form due to filler-to-filler connections [2]. Furthermore, the particle orientation has a huge impact on the thermal conductivity when using anisotropic materials like graphite. Tubes produced by an extrusion process show the natural behaviour of particle alignment in melt flow direction leading to poor thermal conductivities in radial (through-wall) direction. A special extrusion process allows high filler contents and the orientation of filler particles in the polymer matrix to enhance the thermal conductivity in radial direction. More detailed information about the enhanced thermal and mechanical properties and the heat transfer performance of the novel polymer composite tubes is given by Glade et al. [4]. The polymer composite tubes offer opportunities in many fields of heat transfer applications such as industrial water treatment, seawater desalination,

flue gas cooling and thermal processes in the chemical industry [4].

Crystallization fouling often occurs in heat exchangers, especially when using aqueous solutions. The most prevalent type of crystallization fouling is precipitation and deposition of dissolved salts, also referred to as scaling. The solubility of salts exhibiting an inverse solubility, such as calcium sulphate (CaSO_4), calcium carbonate (CaCO_3) and magnesium hydroxide ($\text{Mg}(\text{OH})_2$), decreases with increasing temperature. Therefore, these salts have a tendency to precipitate on heated surfaces, additionally promoted by heterogeneous nucleation mechanisms.

When a new or cleaned heat exchanger is brought into operation, the initially high heat transfer coefficients may remain unchanged for a certain time. The induction period is the period of time observed before the formation of a fouling layer takes place. During this time, nuclei for crystallization are formed. This delay period may last from few seconds to several days [5]. Scale formation on the heat transfer surface creates an additional resistance to heat transfer. The fouling resistance reduces the overall heat transfer coefficient under clean conditions. Thus, it leads to a decrease of the heat duty of an existing heat exchanger or to an additional surface requirement in the design of a new heat exchanger. Over-sizing the heat transfer surface area, fouling mitigation measures, cleaning methods as well as production losses during plant shutdown create considerable capital, operating and maintenance costs.

Operating parameters, solution composition and heat transfer surface characteristics are influencing factors for scaling [6]. In addition to the selection of the heat exchanger type, the proper selection of the heat exchanger material is the second most important point [5]. The main characteristics of the surface with regard to fouling are roughness, hydrophilicity and hydrophobicity, surface free energy, surface charge and chemical inertness. Thus, the choice of heat transfer surface material affects the wettability, the adhesion forces between surface and deposit as well as the induction period of fouling [7].

Fouling on metal surfaces has been extensively studied (e.g., [8]). Although there is a growing interest in polymer materials for heat exchangers, fouling data for polymer surfaces are very limited [9]. An overview of previous studies about crystallization fouling on polymer surfaces compared to metal surfaces is given by Glade et al. [4]. There are contrary reports on the fouling propensity of polymer surfaces compared to metal surfaces. Some reports (e.g., [10-12]) showed that the fouling propensity of polymer surfaces is higher than or the same as that of metal surfaces, while other reports (e.g., [9, 13, 14]) showed that polymer surfaces are less prone to fouling compared to metal

surfaces. Surface roughness and interfacial energies are assumed to be decisive factors. Al-Janabi and Malayeri [15] summarized that there is no consensus among investigators on the effect of surface energy as well as the interaction energies on fouling propensity. However, it is generally assumed that the adhesive strength between the deposit and the heat transfer surface is lower for polymer surfaces than for metal surfaces (e.g., [5, 14]).

The objectives of this study are to gain knowledge of the crystallization fouling propensity of the thermally conductive polymer composite tubes and to compare their fouling tendency to common metal tubes.

EXPERIMENTAL

The crystallization fouling experiments were performed in a stirred vessel and in a falling film test rig with electrical heating. Falling film heat exchangers are widely used in desalination, industrial water treatment and brine concentration applications. Calcium sulphate and calcium carbonate were applied as model foulants.

Test Rigs

A schematic diagram of the stirred vessel test rig is shown in Fig. 1. An electrically heated tube is immersed into an aqueous salt solution in a stirred vessel. The solution is stirred with a 4-bladed propeller stirrer. A cylindrical heating cartridge is inserted into an aluminium cylinder which in turn is inserted into the tube with heat-conducting paste. The temperature of the aluminium cylinder is kept constant with a PID controller and the heating power is measured. The bulk temperature of the solution is controlled with a thermostatic bath. Temperatures are measured in the wall of the aluminium cylinder and in the bulk solution with Pt100 thermometers.

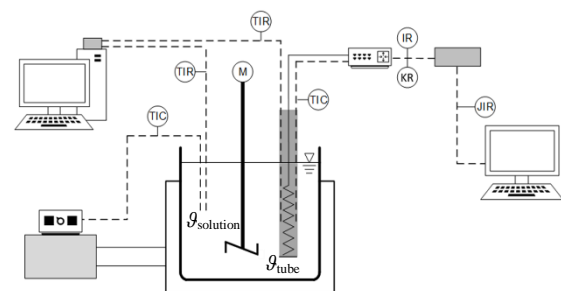


Fig. 1. Schematic diagram of the stirred vessel test rig.

Furthermore, experiments were performed in a falling film test rig, as shown in Fig. 2. Main part of the test rig is a falling film unit fitted with two horizontal tubes, which can be removed from the tube sheets in order to test different tube materials and to analyse the adherent scale. The test solution is evenly distributed onto the upper tube by an overflow weir and trickles down by gravity forming a thin liquid film on the outside of the tubes. A

cylindrical heating cartridge is inserted into an aluminium cylinder which in turn is inserted into the second tube with heat-conducting paste. The temperature of the aluminium cylinder is kept constant with a PID controller and the heating power is measured. The temperature of the test solution distributed onto the first tube is controlled with a thermostat. Temperatures are measured with Pt100 thermometers.

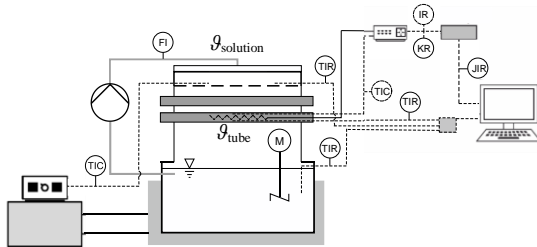


Fig. 2. Schematic diagram of the falling film test rig.

Tube Materials

Experiments were performed with thermally conductive polymer composite and stainless steel tubes. The polypropylene-graphite composite (in the following referred to as PP-GR) and the polyphenylene sulphide-graphite composite (in the following referred to as PPS-GR) had a filler content of 50 vol%. PP-GR, PPS-GR and modified PPS-GR tubes based on a different formulation (marked with PPS-GR-M) were tested and compared to stainless steel 1.4462 (in the following referred to as duplex) and stainless steel 1.4404 (in the following referred to as 316L). In order to study the effects of a surface treatment which improves tube wetting, PP-GR, PPS-GR and PPS-GR-M tubes with surface treatment were applied (surface-treated tubes are marked with trd). The tube data are summarized in Table 1.

Table 1. Tube data (outside diameter $d_o = 24$ mm).

Material	$s /$ mm	$k /$ W/(m K)	$R_a /$ μm	$\gamma /$ mJ/m ²
PP-GR 1.5	1.5	13	0.37 ± 0.06	24.5 ± 0.2
PP-GR 1.5 trd	1.5	13	0.39 ± 0.07	41.3 ± 0.4
PP-GR 1.25 trd	1.25	15	0.58 ± 0.08	31.3 ± 1.1
PPS-GR 1.5	1.5	13	0.48 ± 0.07	39.3 ± 1.8
PPS-GR 1.5 trd	1.5	13	0.56 ± 0.10	48.3 ± 4.0
PPS-GR-M 1.5	1.5	13	0.50 ± 0.09	30.5 ± 0.8
PPS-GR-M 1.5 trd	1.5	13	0.54 ± 0.08	40.3 ± 1.6
316L 1.0	1.0	16	0.52 ± 0.08	28.4 ± 1.8
Duplex 0.7	0.7	15	0.43 ± 0.13	39.6 ± 3.3

The composite and the metal tubes had an outside diameter of 24 mm. The tube wall thickness

was 1.25 or 1.5 mm for PP-GR, 1.5 mm for PPS-GR and PPS-GR-M, 1.0 mm for 316L and 0.7 mm for duplex. In the stirred vessel test rig, the submerged tube length was about 170 mm and the heated tube length amounted to 100 mm. In the falling film test rig, the wetted tube length was 300 mm, while the heated tube length amounted to 100 mm. New tubes, which were not exposed to water before, were used in each experiment.

The thermal conductivities of the polymer composite tubes were measured using a transient hot bridge (THB) method [4]. As shown in Table 1, the thermal conductivities k of the polymer composite tubes were comparable to those of the duplex and 316L tubes.

The tubes were employed with their typical surface topography as delivered by the tube suppliers. Surface roughness parameters, such as the average arithmetic roughness R_a , were measured at eight positions along and around the tubes using a tactile stylus unit (MarSurf GD25, Mahr GmbH, Göttingen).

The advancing contact angles were measured on top of the tubes using a drop shape analysis (DSA) instrument (contact angle measuring system G2, KRÜSS GmbH, Hamburg). The surface free energy was determined on the basis of the contact angle measurements with three test liquids (water, diiodomethane and ethylene glycol) and Young's equation. The solid/liquid interfacial free energy between tube surface and droplet in Young's equation was calculated using the geometric mean approach [16]. Contact angles were measured five times on each tube.

Test Solutions and Test Procedure

Both calcium sulphate and calcium carbonate are the predominant foulants in a variety of heat transfer applications.

In the stirred vessel test rig, experiments were performed with 4 litres of a calcium sulphate solution having an initial concentration of $c_{0,\text{CaSO}_4} = 25$ mmol/L. The calcium sulphate solution was prepared by mixing Na_2SO_4 and $\text{CaCl}_2 \cdot 2\text{H}_2\text{O}$ in deionised and degassed water. The solution bulk temperature was kept at 42 °C and the tube temperature was adjusted to 75 °C for all tube materials. The stirrer had a rotational speed of 2 revolutions per second. The experiments were performed for a test period of 48 hours.

In the falling film test rig, experiments were conducted with 8 litres of a mixed solution containing calcium sulphate and calcium carbonate. The solution had an initial CaSO_4 concentration of $c_{0,\text{CaSO}_4} = 30$ mmol/L and an initial CaCO_3 concentration of $c_{0,\text{CaCO}_3} = 2$ mmol/L. The salt solution containing calcium sulphate and calcium carbonate was prepared by mixing Na_2SO_4 , NaHCO_3 and $\text{CaCl}_2 \cdot 2\text{H}_2\text{O}$ in deionised water. The initial pH value was adjusted to $\text{pH}_0 = 8.0$ (at 42 °C)

by adding sodium hydroxide solution. ACS reagent grade chemicals were used. The solution temperature was kept at 42 °C and the tube temperature amounted to 85 °C. The wetting rate, which is the mass flow rate per unit tube length, is an important parameter in falling film flow applications. A wetting rate of 0.12 kg/(s m), which is often applied in desalination and water treatment plants, was chosen. The experiments were performed for a test period of 24 hours.

The saturation index SI is a useful quantity to determine whether an aqueous solution is saturated (SI = 0), unsaturated (SI < 0) or supersaturated (SI > 0) with respect to the given mineral. The saturation index is defined as the decadic logarithm of the ratio of the ion activity product to the solubility product as given by

$$SI = \log_{10} \left(\frac{\prod_i a_i^{v_i}}{K_{SP}} \right). \quad (1)$$

The computer program PHREEQC [17], which is designed to perform aqueous geochemical calculations, was used with the database WATEQ4F for saturation index calculations.

Major crystal modifications of calcium sulphate are dihydrate (gypsum, $\text{CaSO}_4 \cdot 2\text{H}_2\text{O}$), hemihydrate ($\text{CaSO}_4 \cdot \frac{1}{2}\text{H}_2\text{O}$) and anhydrite (CaSO_4). Hemihydrate has a higher solubility and becomes important at higher temperatures which are not considered here.

Depending on the scaling conditions, calcium carbonate may precipitate in three different anhydrous crystalline forms: calcite, aragonite, and vaterite. The three polymorphs have markedly different crystallographic characteristics, crystal growth habits, and solubilities. Vaterite is a thermodynamically unstable polymorph of CaCO_3 .

Figure 3 shows the saturation index of gypsum and anhydrite in the calcium sulphate test solution with an initial concentration of 25 mmol/L in dependence of temperature.

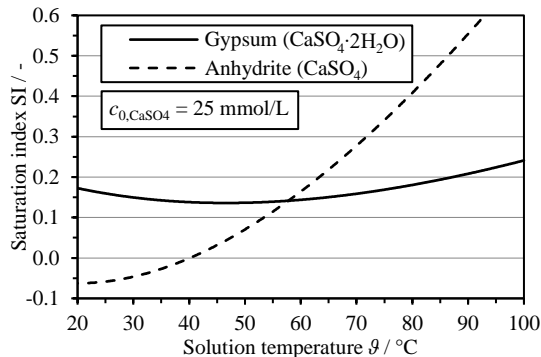


Fig. 3. Saturation index of gypsum and anhydrite in the test solution with the initial concentration of $c_{0,\text{CaSO}_4} = 25$ mmol/L in dependence of temperature.

In the experiments, the solution was supersaturated with CaSO_4 in the bulk at a temperature of 42 °C and at the tube surface with a temperature of 75 °C, as illustrated in Fig. 3.

Figure 4 shows the saturation index of gypsum, anhydrite, calcite and aragonite in the mixed salt test solution at a pH value of 8.0 (at 42 °C) in dependence of temperature. In the experiments, the solution was supersaturated with CaSO_4 and CaCO_3 in the bulk at a temperature of 42 °C and at the tube surface with a temperature of 85 °C.

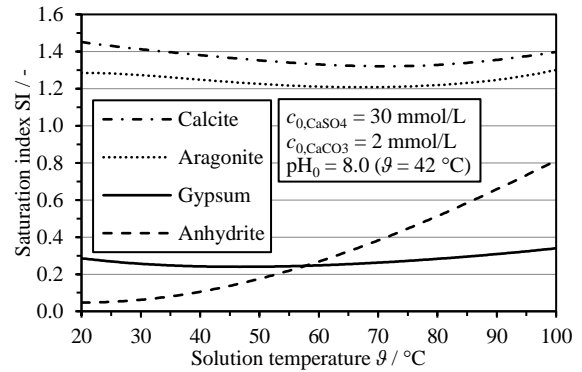


Fig. 4. Saturation index of gypsum and anhydrite as well as calcite and aragonite in the test solution with the initial concentrations of $c_{0,\text{CaSO}_4} = 30$ mmol/L and $c_{0,\text{CaCO}_3} = 2$ mmol/L in dependence of temperature.

From a thermodynamic point of view, anhydrite is the least soluble and, therefore, the most stable CaSO_4 crystal form when elevated temperatures are considered. However, anhydrite nucleation is a slow process [18] and, thus, gypsum crystals are often formed.

The formation of calcium carbonate polymorphs in aqueous supersaturated solutions is strongly influenced by the temperature and by the presence of dissolved cationic and anionic species [19]. Although calcite is less soluble and, hence, the thermodynamically more stable crystal modification, CaCO_3 scales formed at elevated temperatures often consist of aragonite [20].

Test Evaluation

As the temperature difference between the tube and the test solution is kept constant, the build-up of a fouling layer on the heat transfer surface introduces an additional heat transfer resistance, which reduces the heat transfer rate. Thus, the heating power decreases over time. The fouling resistance R_f is determined as

$$R_f = A_o \left(\frac{\vartheta_{\text{tube},t} - \vartheta_{\text{solution},t}}{Q_t} - \frac{\vartheta_{\text{tube},0} - \vartheta_{\text{solution},0}}{Q_0} \right), \quad (2)$$

whereas $\vartheta_{\text{tube},t}$ and $\vartheta_{\text{tube},0}$ are the temperatures measured inside the tube at the time t and at the initial time, respectively, $\vartheta_{\text{solution},t}$ and $\vartheta_{\text{solution},0}$ are

the solution bulk temperatures at the time t and at the initial time, respectively, \dot{Q}_t and \dot{Q}_0 are the heat transfer rates at the time t and at the initial time, respectively, and A_0 is the outside heat transfer surface area of the heated tube. The heat transfer rates were set equal with the measured power outputs of the heating cartridge.

In practice, it is common to use the cleanliness factor CF given by

$$CF = \frac{U_f}{U_0} \quad (3)$$

with the overall heat transfer coefficient U_f under fouled conditions and the overall heat transfer coefficient U_0 under clean conditions. The use of the cleanliness factor is helpful in comparing the condition of the heat exchanger during service to clean conditions.

Determining the fouling resistances for each tube material gives a fouling curve over time from which three characteristic fouling parameters can be obtained. At the beginning of each experiment an induction period can be observed where no significant reduction of the heat transfer takes place. The slope of the following increase of the fouling resistance corresponds to the fouling rate. Furthermore, an asymptotic fouling resistance is reached at the end of the experiments.

RESULTS

In the following, the results obtained in the stirred vessel and in the falling film test rig are presented.

Stirred Vessel Test Rig

Figure 5 shows the fouling resistance over time for the polymer composite tubes and the duplex stainless steel tube obtained with a CaSO_4 solution in the stirred vessel test rig.

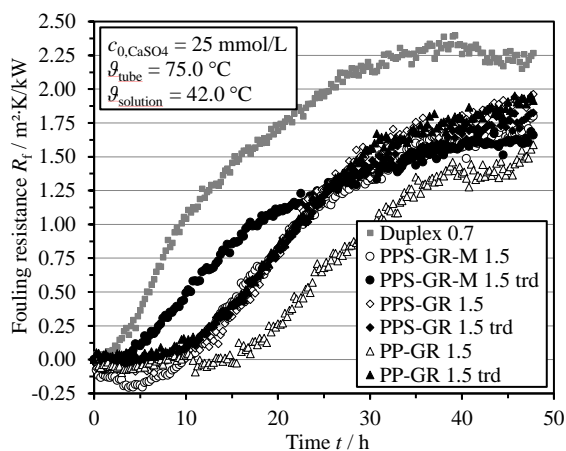


Fig. 5. Fouling resistance of different tube materials with CaSO_4 solution in the stirred vessel test rig.

The fouling resistance shows an asymptotic behaviour over time. The rate of deposit growth can

be regarded as the difference between the deposition and removal rates. If the net deposition approaches zero at later stages, asymptotic behaviour will be obtained. As shown in Fig. 5, the induction periods of fouling were different for the tube materials. The induction period of the duplex stainless steel was found to be only 1.9 hours, while the induction periods of the polymer composite surfaces were considerably higher, namely about 9.9 hours for PPS-GR-M, 10.4 hours for PPS-GR and 15.7 hours for PP-GR. The polymer composite tubes with surface treatment showed shorter induction periods than the respective polymer composite tubes without surface treatment. However, the induction periods of the surface-treated polymer tubes were still notably higher than the one of the duplex tube. Furthermore, the polymer composite tubes exhibited lower fouling rates than the duplex tube, and the asymptotic fouling resistance was higher for duplex stainless steel than for PPS-GR and PPS-GR-M, and it was the lowest for the PP-GR tube.

The cleanliness factor is depicted in Fig. 6. After a short induction period of 1.9 hours, the overall heat transfer coefficient obtained with the duplex stainless steel tube decreased rapidly to only 35.1 % of the initial overall heat transfer coefficient under clean conditions. For PPS-GR-M, PPS-GR and PP-GR, the overall heat transfer coefficients started to decrease after 9.9 hours, 10.4 hours and 15.7 hours (induction periods), respectively, and dropped down to 48.3 %, 46.0 % and 57.7 % of their initial values, respectively.

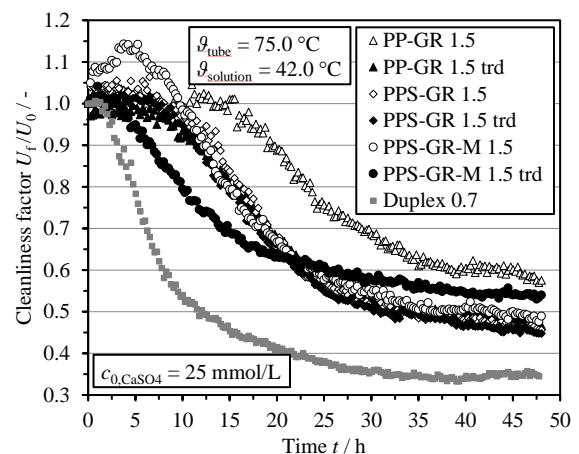


Fig. 6. Cleanliness factor of different tube materials with CaSO_4 solution in the stirred vessel test rig.

Under special circumstances where the surface is initially smooth and the deposit formation increases the surface roughness, the convective heat transfer can be enhanced. The increase in roughness may actually reduce the net system resistance and one may encounter negative values for the fouling resistance during the initial period [7]. Slightly negative values for the fouling resistance and, thus, values higher than one for the cleanliness factor can be seen in Figs. 5 and 6 during the initial period.

Falling Film Test Rig

Figure 7 shows the fouling resistance over time for the polymer composite tubes and the stainless steel tubes obtained with a mixed CaSO_4 and CaCO_3 solution in the falling film test rig. Similar to the results obtained in the stirred vessel test rig, the fouling resistance shows an asymptotic behaviour over time. The induction periods observed with the polymer composite tubes were longer, the fouling rates and the asymptotic fouling resistances were lower compared to both the duplex and the 316L stainless steel tubes.

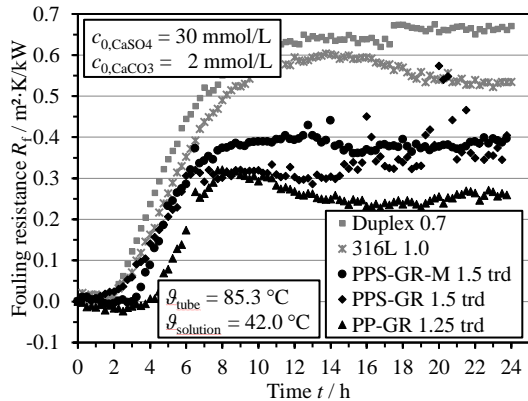


Fig. 7. Fouling resistance of different tube materials with mixed salt solution in the falling film test rig ($\Gamma = 0.12 \text{ kg}/(\text{s m})$).

Figure 8 shows the cleanliness factor over time for the polymer composite tubes and the stainless steel tubes in the falling film test rig.

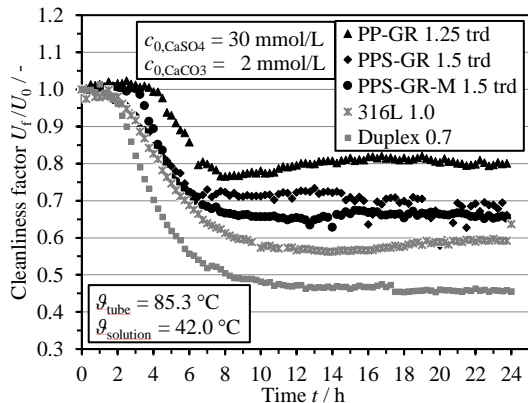


Fig. 8. Cleanliness factor of different tube materials with mixed salt solution in the falling film test rig ($\Gamma = 0.12 \text{ kg}/(\text{s m})$).

After a short induction period of 1.8 h, the overall heat transfer coefficient dramatically decreases to only 45.7 % of its initial value in the test run with the duplex tubes. Similarly, the 316L stainless steel tubes show a short induction period of 2.2 h as well as a strong reduction of the overall heat transfer coefficient to 59.2 % of its initial value. In comparison to the metal tubes, the polymer

composite tubes exhibit longer induction periods. Furthermore, the reduction of the overall heat transfer coefficient over time is notably lower. For PPS-GR 1.5 trd, PPS-GR-M 1.5 trd and PP-GR 1.25 trd, the overall heat transfer coefficients started to decrease after 2.1 hours, 3.1 hours and 4.1 hours (induction periods), respectively, and dropped down to 68.0 %, 65.4 % and 80.0 % of their initial values, respectively.

Figure 9 and Figure 10 summarize the induction periods and the asymptotic cleanliness factors obtained with the polymer composite tubes and the stainless steel tubes in the stirred vessel and in the falling film test rig, respectively.

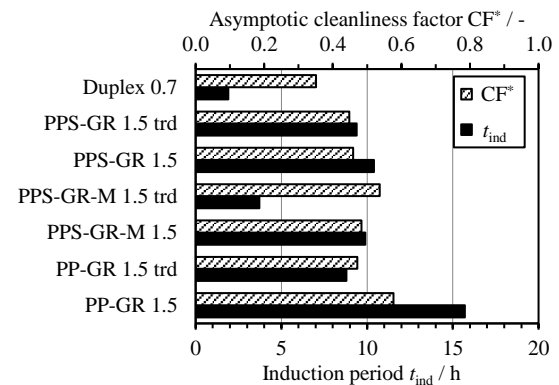


Fig. 9. Summary of asymptotic cleanliness factors and induction periods in the stirred vessel tests.

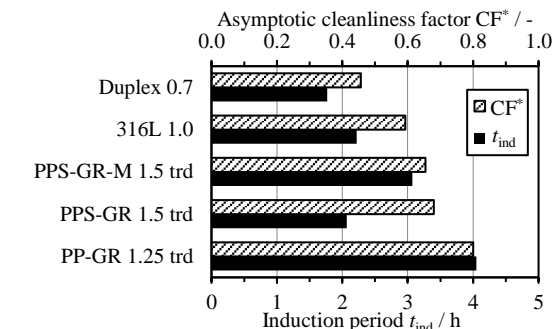


Fig. 10. Summary of asymptotic cleanliness factors and induction periods in the falling film tests.

DISCUSSION

The results suggest that the crystallization fouling propensity of the PP-GR, PPS-GR and PPS-GR-M tube surfaces in contact with a CaSO_4 solution or a mixed CaSO_4 and CaCO_3 solution is lower than that of the stainless steel surfaces under the same test conditions. The PP-GR tubes showed a lower fouling propensity than the PPS-GR tubes.

Modern anti-fouling strategies are based on approaches increasing the duration of the induction period and, hence, several attempts have been made to decrease the adhesive strength between crystals and heat transfer surface [21]. Sheikholeslami [7] stated that the best way to mitigate fouling is to prolong the induction period for the longest time possible.

Surface roughness is believed to enhance nucleation and to increase the contact surface area which in turn increases adhesion [5, 7]. Both PP-GR, which had a slightly lower surface roughness than duplex, and PPS-GR, which had a slightly higher surface roughness than duplex (see Table 1), showed a notably higher induction period. The surface roughness is most likely not the decisive factor for the stronger scale formation on the metal tubes. Since the scale layer can be detached more easily from the polymer tubes than from the metal tubes, it is assumed that the adhesive strength between scale layer and substrate surface is lower for the polymer composite tubes, which would increase the removal rate relative to the rate of deposition and, thus, prolong the induction period. It can be assumed that there are further surface characteristics such as energetic properties lowering the adhesive strength and increasing the induction period for the polymer composite materials.

So far, no simple correlation between surface free energy or surface roughness and fouling behaviour has been confirmed [22], but several studies displayed a strong dependence between surface free energy or surface roughness and crystallization fouling. Zhao and Müller-Steinhagen [23] summarized that there are a number of contrary reports on the effects of surface energy on fouling behaviour. Some reports showed that foulants attached preferentially to surfaces with high surface energy, while other reports showed that foulants attached preferentially to surfaces with low surface energy. Numerous studies also indicated there was no relationship between surface energy/wettability and fouling behaviour. It has long been suspected that poorest foulant adhesion occurs on surfaces with low surface energies and that low energy surfaces were more resistant to build-up of fouling and easier to clean [22, 23]. Siebeneck [24] also summarized that no clear-cut correlation which successfully links fouling effects to energetic surface properties has been found.

The comparison of surface free energy data in Table 1 and the fouling behaviour in Figs. 9 and 10 confirms that there is no simple correlation between the surface free energy and the fouling behaviour. The polymer composite tubes which have a lower surface free energy, e.g. PP-GR, and those which have a higher surface free energy, e.g. surface-treated PPS-GR, than the stainless steel tubes exhibit a longer induction period than the metal tubes. However, surface-treated polymer composite tubes having a higher surface free energy than the respective untreated tubes show a shorter induction period than the untreated tubes.

Since the crystalline deposit also influences molecular interaction at the interface crystal/heat transfer surface, it has to be taken into account. Förster [10] developed an interfacial defect model based on the relationship between wetting

characteristics and adhesive strength. Förster [10] found that the model is valid for metal surfaces, while in case of polymer surfaces a significant deviation was observed. For scale formation on polymer surfaces, Dreiser [14] showed that scale quantity strongly depends on the surface free energy difference between crystalline deposit and heat transfer surface. Dreiser [14] reported that a lower interfacial energy difference results in stronger interactions, which implicates both a shorter induction period and a higher amount of final scale deposit. Al-Janabi and Malayeri [15] showed that the total surface energy and the Lifshitz-van der Waals component are not sufficient to evaluate the deposition process. They found that the Lewis acid-base interaction energy has a strong implication on the adhesion process and must be taken into account.

CONCLUSION

Thermally conductive polymer composite tubes have been developed as an alternative material for heat exchangers in harsh environments. The fouling behaviour of the polymer composite tubes was studied in a stirred vessel and a falling film test rig with electrical heating and compared to common duplex and 316L stainless steel tubes. The novel polymer composite tubes showed a lower crystallization fouling tendency compared to the stainless steel tubes. The induction period was longer and the reduction of the overall heat transfer coefficient over time was notably lower compared with the duplex and the 316L stainless steel tubes.

The excellent chemical resistance of the polymer composite tubes to strong acids and alkaline media, low weight, high degree of freedom in shaping and promising results of fouling studies compared to metals offer benefits and open up cost-efficient opportunities for the construction of polymer composite heat exchangers in various industries such as chemical, oil and gas, power generation, water treatment and desalination industries.

In future work, a more detailed study of the influence of interfacial interactions on crystallization fouling will be performed to improve the knowledge of the complex relationships.

NOMENCLATURE

a_i	activity of species i , dimensionless
A	heat transfer area, m^2
CF	cleanliness factor, dimensionless
d	tube diameter, m
k	thermal conductivity, $W/(m\ K)$
K_{SP}	solubility product, dimensionless
\dot{Q}	heat transfer rate, W
R_a	average arithmetic roughness, m
R_f	fouling resistance, $m^2\ K/W$
s	tube wall thickness, m
SI	saturation index, dimensionless
t	time, h

U	overall heat transfer coefficient, W/(m ² K)
γ	surface free energy, J/m ²
Γ	wetting rate, kg/(s m)
ϑ	temperature, °C
ν	stoichiometric number, dimensionless

Subscript

0	initial, clean
f	fouled
ind	induction
o	outside
t	at time t

Superscript

*	asymptotic value
---	------------------

REFERENCES

- [1] Cevallos, J. G., Bergles, A. E., Bar-Cohen, A., Rodgers, P., and Gupta, S. K., Polymer Heat Exchangers – History, Opportunities, and Challenges, *Heat Transfer Engineering*, vol. 33, no. 13, pp. 1075-1093, 2012.
- [2] Chen, H., Ginzburg, V. V., Yang, J., Yang, Y., Liu, W., Huang, Y., Du, L., and Chen, B., Thermal Conductivity of Polymer-based Composites: Fundamentals and Applications, *Progress in Polymer Science*, vol. 59, pp. 41-85, 2016.
- [3] Chen, X., Su, Y., Reay, D., and Riffat, S., Recent Research in Polymer Heat Exchangers – A Review, *Renewable and Sustainable Energy Reviews*, vol. 60, pp. 1367-1386, 2016.
- [4] Glade, H., Orth, T., and Moses, D., Polymer Composite Heat Exchangers, in *Innovative Heat Exchangers*, eds. H.-J. Bart, and S. Scholl, pp. 53-116, Springer International Publishing AG, Cham, 2018.
- [5] Müller-Steinhagen, H., Fouling of Heat Exchanger Surfaces, in *VDI Heat Atlas*, ed. VDI-GVC, pp. 79-104, Springer, Berlin, 2010.
- [6] Zhao, X., and Chen, X. D., A Critical Review of Basic Crystallography to Salt Crystallization Fouling in Heat Exchangers. Proc. *International Conference on Heat Exchanger Fouling and Cleaning*, Crete Island, 2011.
- [7] Sheikholeslami, R., *Fouling in Membranes and Thermal Units – A Unified Approach – Its Principles, Assessment, Control and Mitigation*. Desalination Publications, L'Aquila, 2007.
- [8] Müller-Steinhagen, H., Modellierung der Ablagerungsbildung in Wärmeübertragern, ESYTEC Energie- und Systemtechnik GmbH, Erlangen, 2000.
- [9] Wu, Z., Francis, L. F., and Davidson, J. H., Scale Formation on Polypropylene and Copper Tubes in Mildly Supersaturated Tap Water, *Solar Energy*, vol. 83, pp. 636-645, 2009.
- [10] Förster, M.L., Verminderung des Kristallisationsfouling durch gezielte Beeinflussung der Grenzfläche zwischen Kristallen und Wärmeübertragungsfläche, Ph.D. thesis, Technische Universität Braunschweig, 2001.
- [11] Wang, Y., Davidson, J. H., and Francis, L. F., Scaling in Polymer Tubes and Interpretation for Use in Solar Water Heating Systems, *Journal of Solar Energy Engineering*, vol. 127, pp. 3-14, 2005.
- [12] Wu, Z., Davidson, J. H., and Francis, L. F., Effect of Water Chemistry on Calcium Carbonate Deposition on Metal and Polymer Surfaces, *Journal of Colloid and Interface Science*, vol. 343, pp. 176-187, 2010.
- [13] Kazi, S. N., Duffy, G. G., and Chen, X. D., Mineral Scale Formation and Mitigation on Metals and Polymeric Heat Exchanger Surface, *Applied Thermal Engineering*, vol. 30, pp. 2236-2242, 2010.
- [14] Dreiser, C., Falling Liquid Film Enhancement, Fouling Mitigation and Conceptual Design of Polymer Heat Exchangers, Ph.D. thesis, Technische Universität Kaiserslautern, Shaker Verlag, Aachen, 2016.
- [15] Al-Janabi, A., and Malayeri, M. R., A Criterion for the Characterization of Modified Surfaces during Crystallization Fouling based on Electron Donor Component of Surface Energy, *Chemical Engineering Research and Design*, vol. 100, pp. 212-227, 2015.
- [16] Owens, D. K., and Wendt, R.C., Estimation of the Surface Free Energy of Polymers, *Journal of Applied Polymer Science*, vol. 13, pp. 1741-1747, 1969.
- [17] Parkhurst, D. L., Thorstenson, D. C., Plummer, L. N., PHREEQE – A Computer Program for Geochemical Calculations, Water-Resources Investigations Report 80-96, U.S. Geological Survey, 1980.
- [18] Hasson, D., Scale Formation and Prevention, in *Scaling in Seawater Desalination – Is molecular modelling the tool to overcome the problem?*, eds. J. Ulrich, and H. Glade, pp. 49-68, Shaker Verlag, Aachen, 2001.
- [19] Morse, J. W., Wang, Q., and Tsio, M. Y., Influences of Temperature and Mg:Ca Ratio on CaCO₃ Precipitates from Seawater, *Geology*, vol. 25, pp. 85-87, 1997.
- [20] Krömer, K., Will, S., Loisel, K., Nied, S., Detering, J., Kempter, A., and Glade, H., Scale Formation and Mitigation of Mixed Salts in Horizontal Tube Falling Film Evaporators for Seawater Desalination, *Heat Transfer Engineering*, vol. 36, pp. 750-762, 2015.

- [21] Förster, M., and Bohnet, M., Modification of Molecular Interactions at the Interface Crystal/Heat Transfer Surface to Minimize Heat Exchanger Fouling, *International Journal of Thermal Science*, vol. 39, pp. 697-708, 2000.
- [22] Zettler, H. U., Wei, M., Zhao, Q., and Müller-Steinhagen, H., Influence of Surface Properties and Characteristics on Fouling in Plate Heat Exchangers, *Heat Transfer Engineering*, vol. 26, pp. 3-17, 2005.
- [23] Zhao, Q., and Müller-Steinhagen, H., Intermolecular and Adhesion Forces of Deposits on Modified Heat Transfer Surfaces, Proc. *4th International Conference on Heat Exchanger Fouling, Fundamental Approaches & Technical Solutions*, Davos, Switzerland, pp. 41-46, 2002.
- [24] Siebeneck, K., Energetic Surface Properties in Crystallization Fouling on Modified Surfaces, Ph.D. thesis, Technische Universität Braunschweig, ICTV-Schriftenreihe, vol. 27, Cuvillier Verlag, Göttingen, 2017.